







# Designing an Integrated CSP-SOE System for Hydrogen Production

Abdullah Ayed Alrwili<sup>1,2,\*</sup> , Khalifa Aliyu Ibrahim<sup>1,3</sup> , Peter King<sup>1</sup> ,  
Ahmed Ali Aldubayyan<sup>1,4</sup> , Yousef Lafi A Alshammari<sup>2,5</sup> , and Zhenhua Luo<sup>1</sup> 

<sup>1</sup>Cranfield University, Energy and Power, Cranfield U.K.

<sup>2</sup>Mechanical Engineering Department, Engineering College, Northern Border University, Saudi Arabia.

<sup>3</sup>Physics department, Kaduna State University, Nigeria.

<sup>4</sup>Department of Mechanical Engineering, College of Engineering, Qassim University, Saudi Arabia.

<sup>5</sup>School of Aerospace, Transport and Manufacturing, Cranfield University, UK.

\*Correspondence: Abdullah Ayed Alrwili, [abdullah.alrwili@cranfield.ac.uk](mailto:abdullah.alrwili@cranfield.ac.uk)

**Abstract.** This paper presents the design, and simulation of a novel concentrated solar power (CSP) system integration with solid oxide electrolysis (SOE) to generate superheated steam required for efficient hydrogen production. The system comprises of 10 parabolic dish collectors, SiSiC cavity receivers, and a heat exchanger with two components. An evaporator and a superheater collectively achieve a high thermal efficiency of 73%. Computational fluid dynamics (CFD) simulations demonstrated that the SiSiC receiver can maintain an air outlet temperature of 1555K, which is 8% more efficient than a similar design reported in the literature. This would facilitate the generation of superheated steam necessary for the SOE process. A water flow rate of 28.8kg/h directly influences the system's hydrogen production capacity, which reaches 2.56kg/h at optimal conditions. The heat exchanger components were designed using Aspen EDR, while the entire system simulation was conducted using Aspen Plus, demonstrating the system's potential to meet industrial standards for sustainable hydrogen production. This article serves as a good reference in investigating the feasibility of CSP-SOE systems as a promising pathway for large-scale renewable hydrogen production.

**Keywords:** Concentrated Solar Power (CSP), Solid Oxide Electrolysis (SOE), Green Hydrogen Production.

## 1. Introduction

The increase in global demand for sustainable energy presents an increasing challenge [1]. Fossil fuels account for 80% of the world's energy consumption, contributing to a concerning rise in carbon emissions and intensifying fears about climate change. Addressing the urgent need for sustainable energy solutions is critical, requiring innovative strategies to mitigate the impacts of climate change while ensuring energy security. International efforts are increasingly focused on expanding the use of renewable energy [2]. Hydrogen is viewed as a promising energy carrier due to its environmentally friendly nature, with the potential to transform the global energy landscape [3]. However, a substantial proportion of hydrogen, approximately 94%, is currently produced from fossil fuels, undermining efforts to reduce carbon emissions [4], [5]. Therefore, it is necessary to produce hydrogen using renewable energy sources to align with global sustainability goals, a process known as green hydrogen production.

Although green hydrogen is an appropriate source of energy for the environment, it faces challenges that limit its production, especially in the aspect of efficiency and cost of the systems [6]. Green hydrogen is mostly produced using water electrolysis [7]. There are different types of electrolysis. Among them, solid oxide electrolysis (SOE) is considered promising in green hydrogen production because it can produce hydrogen with high efficiencies, potentially reaching 70% to 100% [8]. However, one of the main challenges facing SOE is the very high operating temperatures, which range between 973-1273 K. This is considered a major challenge. Therefore, a clean energy source that can generate thermal energy with high efficiencies is required to be integrated with SOE. This challenge can be met using concentrated solar power (CSP) [9]. CSP systems with integrated SOE technology could increase the efficiency of the electrolysis process, reducing operational costs [10]. CSP technology, particularly in the form of parabolic dish and solar tower systems, could achieve the necessary high temperatures, making it an ideal heat-renewable source for SOE.

A wide range of studies have been conducted on CSP-SOE systems integration due to the potential benefits of the technology. Current research into the integration process of CSP with SOE for hydrogen production has shown promising trends and highlighted serious issues. [11] reported a study involving the application of a parabolic trough collector in producing temperatures as high as 1100°C for SOE in Eshtehard City, Iran. The researchers' system was simulated, obtaining an exergy efficiency of 26.81% and a hydrogen production rate of 260 kg/day. The limitations, however, included design assumptions and that the parabolic trough could not cover all heat demands. In [12], it was highlighted that the Seville, Spain station integrated a linear Fresnel reflector with SOE for a hydrogen bus refuelling station, producing over 500 kg/d of hydrogen with a high efficiency of 43.1%. However, it was reported to have problems with optimisation at large-scale production of hydrogen. Another study by [13] considered a solar power plant with SOE and obtained a hydrogen production rate of 5.5 kg/hour at an efficiency of 39.5% without thermal energy storage. Meanwhile, [14] conducted a simulation for an 80 MW solar tower plant in Germany and obtained an estimated 680 kg/hour of hydrogen production with 18% efficiency. [15] conducted a study on using parabolic dishes in compressed air energy storage that produced 41.48 kg/day of hydrogen and reported the power cycle and electrolysis cell efficiencies were 72.69% and 61.70%, respectively. Despite these developments, the energy conversion efficiency of this integrated system is poor, and the overall system efficiency still needs to be improved. These studies provide a receiver design that can improve the system's performance and efficiency. While previous studies have often concentrated on individual components or theoretical models in this integration, this research takes a new approach by optimising each part within a fully integrated system. The system consists of 10 parabolic dish collectors, SiSiC solar cavity receivers, and a central heat exchanger unit, all integrated to produce the required superheated steam for SOE operation. The objective is to enhance thermal efficiency, reduce the need for additional heating, and more effectively reach the high temperatures required for SOE operation. As a result, this research offers a more practical and efficient solution for green hydrogen production, addressing the high-temperature challenges and inefficiencies highlighted in earlier studies.

This paper introduces an innovative design and simulation of a CSP-SOE system. The parabolic dishes and SiSiC receiver are optimised to achieve the required thermal conditions, while the heat exchanger efficiently delivers superheated steam for SOE. This section provides an introduction, while section 2 provides the methodology and discusses the proposed design components. The receiver performance was confirmed through ANSYS Fluent simulations, while the evaporator and superheater performance were verified using Aspen EDR and the whole system was simulated on Aspen Plus to check the feasibility and efficiency of the approach. Section 3 focuses on the results, providing key information for experimentation. Section 4 concludes the paper by providing key information on the viability of CSP-SOE systems as an attractive way for green hydrogen production.

## 2. Methodology

The design of the CSP system integrated with SOE for efficient production of green hydrogen is presented in this section. The CSP system was configured to consist of 10 parabolic dish collectors that focus radiation onto corresponding cavity receivers. The cavity receivers are made from solid silicon carbide, SiSiC, sharing their heat output with a central unit, the heat exchanger containing an evaporator and superheater. A system has been integrated to maximise the capture of solar energy and transfer it efficiently to generate steam at superheated temperatures for producing hydrogen by SOE. The focus areas of this work are the development of the SiSiC cavity receiver, heat exchanger design, and overall system simulation for performance and efficiency.

### 2.1 Parabolic Dish Design

Each parabolic dish collector was designed to concentrate the solar energy onto the aperture of a cavity receiver. The design of the collector follows standard principles, focusing on achieving a high concentration ratio, which is critical for delivering sufficient thermal energy to the receivers. To evaluate the area of the parabolic dish, this equation is applied [16]:

$$Q = A_c I_b \rho \alpha \gamma \quad (1)$$

Where  $Q$  is the required heat to the receiver in W, assumed 5 KW,  $A_c$  is the aperture area of the collector in  $m^2$ ,  $I_b$  is solar irradiation, assumed  $1000 W/m^2$ ,  $\rho$  is the reflectance of the material, and Naugatuck reflectance is 0.95, which is selected for this dish collector [17].  $\alpha$  is the absorptivity of the receiver, and  $\gamma$  is the intercepting factor [18]. A typical value of the intercepting factor ranges from 0.9 to 0.98 [19]. Figure 1 shows the integrated SCP-SOE system.

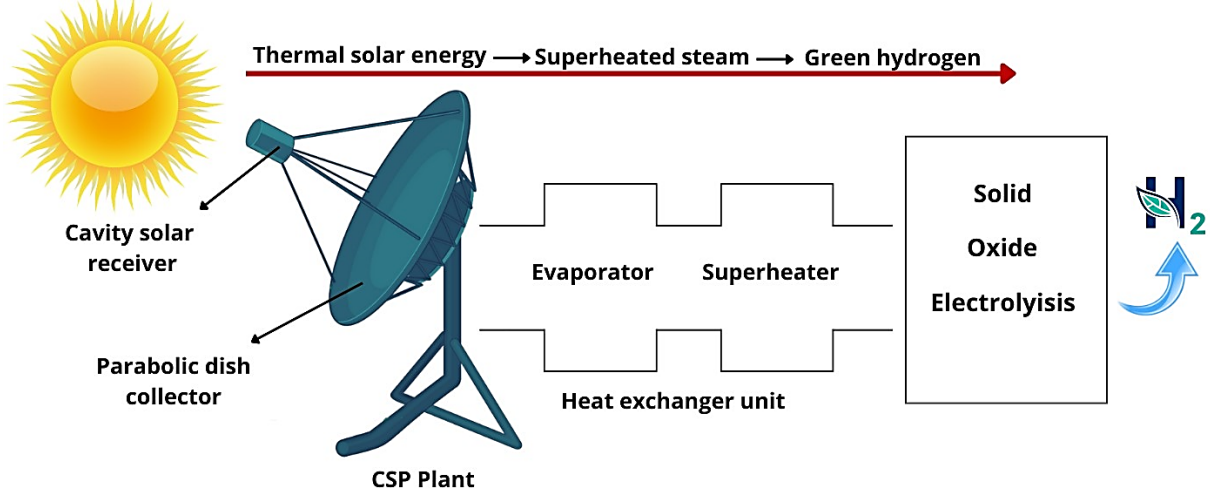


Figure 1. Overview of the CSP-SOE system for green hydrogen production.

### 2.2 Receiver Design

The designed solar receiver was based on similar approaches used in several studies related to cavity receivers [20], [21], [22], [23]. Cavity receivers are characterised by their capability to reach very high temperatures because of their enclosed design, which minimises radiative heat loss and maximises thermal efficiency. This makes them particularly suitable for applications like CSP systems where high operational temperatures are critical. Building on these foundational designs, a cavity receiver has been developed using the thermal properties of solid silicon carbide, SiSiC, known to have excellent thermal conductivity and mechanical strength at elevated temperatures, surrounded by insulation materials to minimise heat losses [17].

shows the receiver materials. Heat absorbed by the receiver,  $Q$ , was obtained using the standard energy balance equation [24]:

$$Q = \dot{m} C_p (T_{out} - T_{in}) \quad (2)$$

Where  $\dot{m}$  is the mass flow rate of air through the receiver,  $C_p$  is the specific heat capacity of air, and  $T_{out}$  and  $T_{in}$  are the outlet and inlet temperatures, respectively. The cavity receiver can be seen in Figure 2.

**Table 1.** The properties of the materials used in the solar receiver.

Receiver Materials	Density	Heat Capacity	Thermal Conductivity	Ref.
Solid silicon carbide Si-SiC	3100	700	120	[25]
Stainless Steel	7954.3	473.62	15.311	[26]
Aluminium	2719	871	202.4	[26]
Cerium Oxide	7215	357.93	0.265 at 773K	[21], [27], [28]
			0.174 at 1273K	
			0.167 at 1773K	
Alumina-Silica	4300	1190	0.055 at 473K	[29]
			0.13 at 873K	
			0.23 at 1273K	

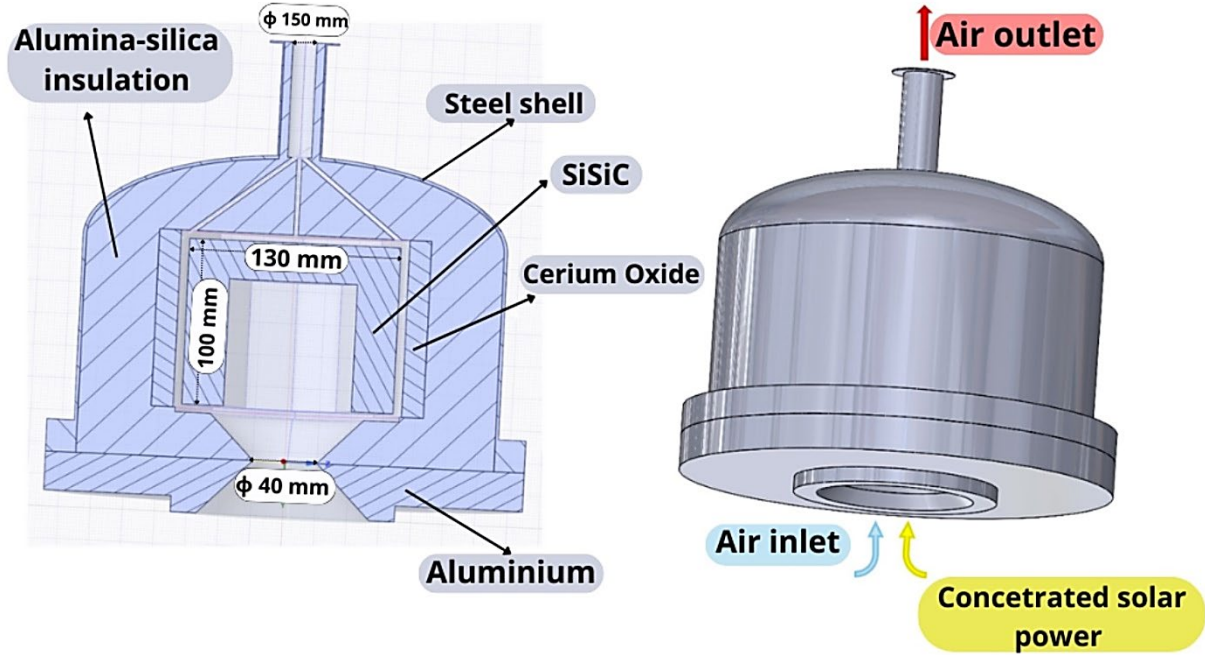


**Figure 2.** 3D model of the solid SiSiC cavity receiver design.

## 2.3 Receiver CFD Modelling in ANSYS Fluent

To evaluate the thermal performance of the SiSiC cavity receiver, Computational Fluid Dynamics (CFD) simulations were conducted using ANSYS Fluent. The simulations aimed to accurately model the heat transfer processes and assess the receiver's efficiency under operational conditions. Table 2 Summarises the key simulation parameters and settings used in the analysis.

**Table 2.** CFD Simulation Parameters for Receiver Modeling in ANSYS Fluent.

Parameter	Value/Setting	Description
<b>Inlet Air Mass Flow Rate</b>	0.00275 kg/s	The mass flow rate of air entering the receiver.
<b>Inlet Air Temperature</b>	300 K	The temperature of the air at the inlet of the receiver.
<b>Solar Irradiation</b>	Uniformly distributed	Assumed uniform solar irradiation across internal surfaces.
<b>Receiver Shell Wall</b>	Convective, heat transfer coefficient: 5 W/m <sup>2</sup> K	Simulates environmental cooling effects.
<b>SiSiC Emissivity and Absorptivity</b>	Emissivity: 0.90, Absorptivity: 0.90	Material properties used for the receiver surface [30], [31].
<b>Insulation</b>	Adiabatic	The insulation surrounding the receiver was modelled as adiabatic.
<b>Turbulence Model</b>	k-omega	Chosen for capturing complex flow patterns and near-wall effects.
<b>Air Properties</b>	Interpolated using Ref-Prop	Temperature-dependent air properties obtained from RefProp [32].
<b>Radiation Model</b>	Discrete Ordinates (DO)	Used for simulating solar radiation within the receiver [33], [34].
<b>Mesh</b>	High-quality mesh with 10,224,979 elements	A mesh independence study confirmed this mesh size's accuracy.
<b>Governing Equations</b>	Navier-Stokes and Energy Equations	Solved using the finite volume method.

## 2.4 Heat Exchanger Design and Simulation

The heat exchanger is a critical component in this integrated system because its function is to convert the captured energy by CSP 10 cavity receivers to the required superheated steam for SOE operation for green hydrogen production. The heat exchanger consists of two parts: an evaporator and a superheater. The design process started with a thermal energy balance to calculate the water mass flow rate that can be generated by the energy coming from CSP, considering the phase change, using this equation:

$$Q = \dot{m} C_p (T_{out} - T_{in}) \quad (2)$$

Next, Using Aspen Plus and Aspen EDR, the heat exchanger was designed in detail. The overall system was modelled in Aspen Plus, while the evaporator and superheater were designed using Aspen EDR. This approach ensured that the heat exchanger met the thermal demands efficiently. Further optimisation was conducted in order to tune very finely the steam mass flow rate so that the system would produce the required steam at the correct temperature and pressure with high efficiency.

## 2.5 Overall System Simulation

The overall system simulation was conducted in Aspen Plus to assess the thermal efficiency and performance of this system. The simulation combined the outputs of the ten parabolic dish receivers, directing the thermal energy to the heat exchanger.

$$\eta_{thermal} = \frac{Q_{useful}}{Q_{Input}} \quad (3)$$

where  $Q_{useful}$  is the energy used for steam generation, and  $Q_{Input}$  is the total solar energy captured.

### 3. Results

This section includes the key findings from the simulation and analysis of the system, like the air outlet temperature from the receiver, mesh independence study, the performance of the heat exchanger, optimisation of the steam mass flow rate, and overall performance of the system.

#### 3.1 Mesh Independence Study

An investigation on mesh independence was carried out to verify the precision of the CFD simulations. The investigation utilised different mesh sizes and observed the air outlet temperature to ascertain the point at which the findings reached a state of convergence. Convergence was attained when the number of elements reached 10,224,979. Further refinement resulted in negligible alterations in the outlet temperature. This verifies that the selected mesh size is adequate for accurately representing the important thermal events occurring in the receiver, hence guaranteeing the dependability of the simulation outcomes. Figure 3 displays the findings of the mesh independence analysis.

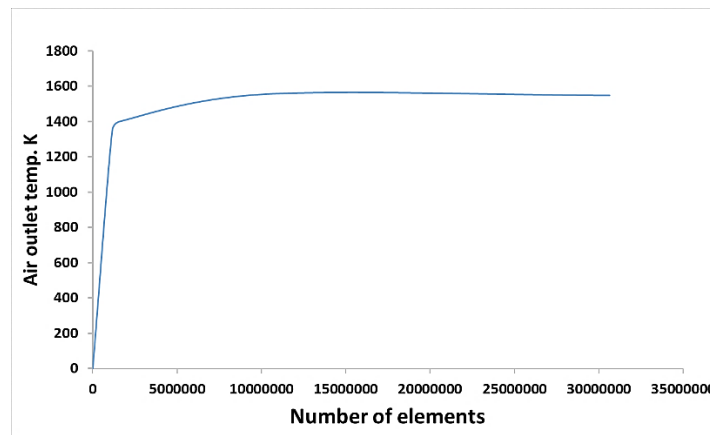
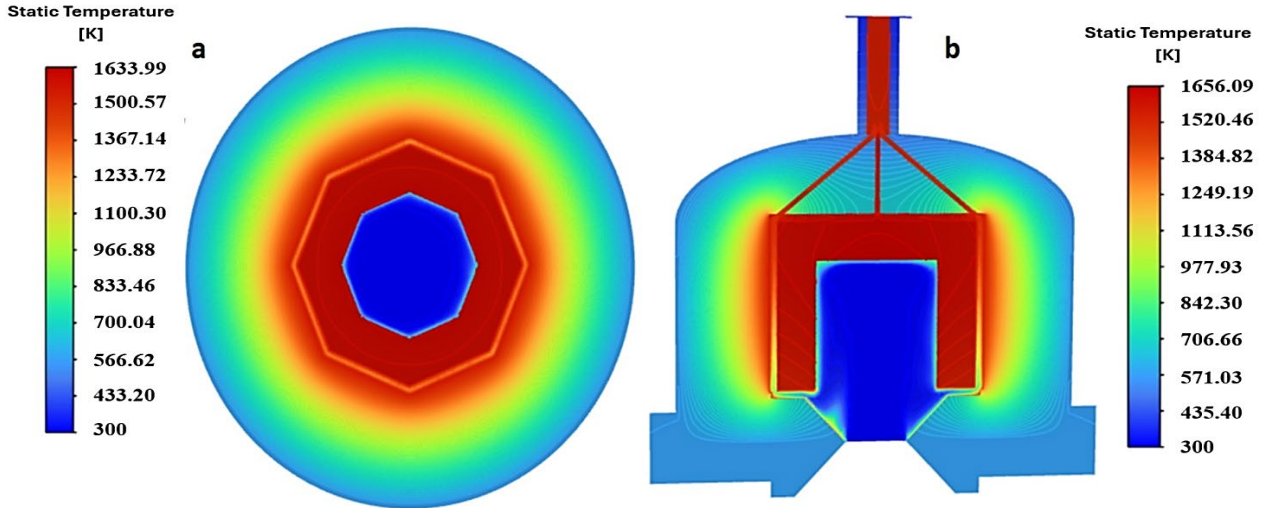


Figure 3. Mesh independence study graph.

#### 3.2 Air Outlet Temperature from the Receiver

The receiver air outlet temperature was evaluated using CFD simulation in Ansys Fluent. The receiver was able to generate an airflow rate of 0.00275 Kg/s at 1555 K. This high temperature at the outlet is critical to be transferred to the next heat exchange process for its efficiency, as this would have a direct influence on the generation of superheated steam required during SOE. This temperature can be held without cutting off, thereby showing the design efficiency of the receiver in capturing and then converting solar energy in the high DNI places during the summer period. Figure 4 shows the temperature distribution concerning the receiver, and it is an indication of effective heat absorption. As shown in Figure 4, it is obvious that the air gains heat mostly in the path between the SiSiC wall and the cerium oxide wall.



**Figure 4.** a. Temperature contour of y-z centre cut-view, b. Temperature contour of x-y centre cut-view of the model from simulation.

### 3.3 Heat Exchanger Inlet and Outlet Temperatures

The performance of the heat exchanger, including both the evaporator and superheater components, was assessed by monitoring each one's inlet and outlet temperatures. Table 3 summarises the calculated areas of the parabolic dish and receiver with the corresponding heat generated.

**Table 3.** Summary of the areas and thermal performance of the system components.

Software/package	Component	Area (m <sup>2</sup> )	Generated Heat (KW)	Number of Units
Manual calculation	Parabolic Dish	5.97	5	10
CFD (Ansys)	Solar Cavity Receiver	0.21	3.86	10
Aspen Plus/Aspen EDR	Evaporator	2.29	22.55	1
Aspen Plus/Aspen EDR	Superheater	2.28	13.29	1

### 3.4 Overall System Performance

The performance of the overall CSP-SOE system is shown in Figure 5. The available heat from the air leaving the receiver is transfer to water to generate steam. The aim was to create superheated steam at the required temperature and pressure for the SOE to generate green hydrogen. It was found that the optimal steam flow rate was obtained to be 28.8 kg/h at 1262K. The effectiveness of the steam generation depends on water flow rate, air temperature from the receiver, and the heat transfer efficiency of the heat exchangers. The system efficiently turned solar energy into superheated steam for hydrogen generation which achieved an efficiency of 73%. In addition, the SOE efficiency hydrogen generation was obtained to be 80%, which generate 2.56Kg/hr of hydrogen. This shows the system's capacity for major hydrogen generation, therefore satisfying industrial criteria for sustainable energy generation. Table 4

show the inlet and outlet temperatures of each step in the system. Determining these temperatures allows to evaluate the efficiency of the heat exchanger, ensuring meeting the required superheated steam temperature for SOE.

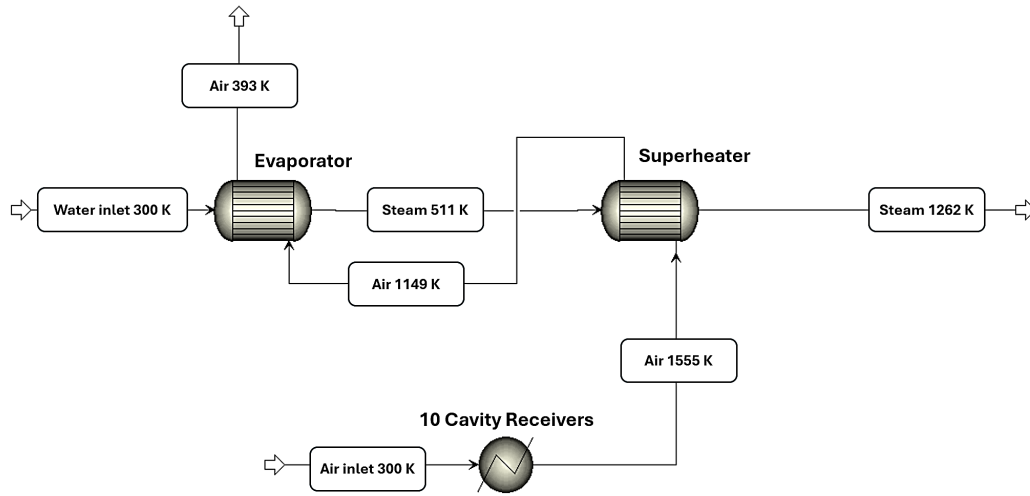


**Figure 5.** Overall system performance schematic from Aspen Plus.

**Table 4.** The fluids inlet and outlet temperatures of each component.

Component	Fluid	Inlet Temperature (K)	Outlet Temperature (K)	Heat duty KW
<b>Solar Cavity Receiver</b>	Air	300	1555	
<b>Superheater</b>	Air (hot fluid)	1555	1148	13.29
	Steam (cold fluid)	551	1262	
<b>Evaporator</b>	Air (hot fluid)	1148	393	22.55
	Water (cold fluid)	300	511	

## 4. Conclusion

This study presents the design, and simulation of a novel CSP-SOE system aimed at efficient superheated steam generation for SOE to enhance green hydrogen production. The integrated system, comprising 10 parabolic dish collectors, SiSiC cavity receivers, and a dual-component heat exchanger, demonstrated a high overall thermal efficiency of 73%. The integrated CSP system was able to produce a superheated steam flow rate of 28.8kg/h at 1262K, leading to 2.56kg/h of green hydrogen. A key novelty of this research lies in the application of solid silicon carbide (SiSiC) in the cavity receiver design, which, through CFD simulations, was shown to maintain a high air outlet temperature of 1555K, critical for the downstream heat exchange process. The optimisation of the water flow rate and the integration of system components in Aspen Plus confirmed the system's capability to meet industry standards for sustainable green hydrogen production. The findings of this study provide important knowledge on the potential of CSP-SOE systems for large-scale hydrogen production. The study serves as a good reference for further research on the technical feasibility of CSP-SOE systems.

## Data availability statement

The data substantiating the findings of this paper can be obtained by contacting the authors.

## Author contributions

**Abdullah Ayed Alrwili:** Methodology, Investigation, Software, Analysing, Writing original draft. **Khalifa Aliyu Ibrahim:** Investigation, Visualization, Software, Writing – review & editing. **Peter King:** Investigation, Supervision, Resources. **Ahmed Ali Aldubayyan:** Writing – review & editing. **Yousef Lafi A Alshammari:** Writing – review & editing. **Zhenhua Luo:** Investigation, Supervision, Resources, Writing review & editing.

## Competing interests

The authors declare no competing interests.

## Acknowledgement

The authors extend their appreciation to the Deanship of Scientific Research at Northern Border University, Arar, KSA for funding this research work through the project number "NBU-SAFIR-2024".

## References

- [1] M. Jefferson, "A global energy assessment," WIREs Energy and Environment, vol. 5, no. 1, pp. 7–15, Jan. 2016, doi: [10.1002/wene.179](https://doi.org/10.1002/wene.179).
- [2] "IRENA – International Renewable Energy Agency." Accessed: Aug. 19, 2024. [Online]. Available: <https://www.irena.org/>
- [3] P. Cheekatamarla, "Hydrogen and the Global Energy Transition—Path to Sustainability and Adoption across All Economic Sectors," Energies (Basel), vol. 17, no. 4, p. 807, Feb. 2024, doi: [10.3390/en17040807](https://doi.org/10.3390/en17040807).
- [4] P. Breeze, "Power System Energy Storage Technologies," in Power Generation Technologies, Elsevier, 2019, pp. 219–249. doi: [10.1016/B978-0-08-102631-1.00010-9](https://doi.org/10.1016/B978-0-08-102631-1.00010-9).
- [5] Q. Hassan, S. Algburi, A. Z. Sameen, H. M. Salman, and M. Jaszczur, "Green hydrogen: A pathway to a sustainable energy future," Int J Hydrogen Energy, vol. 50, pp. 310–333, Jan. 2024, doi: [10.1016/j.ijhydene.2023.08.321](https://doi.org/10.1016/j.ijhydene.2023.08.321).
- [6] B. S. Zainal et al., "Recent advancement and assessment of green hydrogen production technologies," Renewable and Sustainable Energy Reviews, vol. 189, p. 113941, Jan. 2024, doi: [10.1016/j.rser.2023.113941](https://doi.org/10.1016/j.rser.2023.113941).
- [7] L. Wang, W. Liu, H. Sun, L. Yang, and L. Huang, "Advancements and Policy Implications of Green Hydrogen Production from Renewable Sources," Energies (Basel), vol. 17, no. 14, p. 3548, Jul. 2024, doi: [10.3390/en17143548](https://doi.org/10.3390/en17143548).
- [8] W. DONITZ, "High-temperature electrolysis of water vapor?status of development and perspectives for application," Int J Hydrogen Energy, vol. 10, no. 5, pp. 291–295, 1985, doi: [10.1016/0360-3199\(85\)90181-8](https://doi.org/10.1016/0360-3199(85)90181-8).
- [9] Y. Zheng, Z. Chen, and J. Zhang, "Solid Oxide Electrolysis of H<sub>2</sub>O and CO<sub>2</sub> to Produce Hydrogen and Low-Carbon Fuels," Electrochemical Energy Reviews, vol. 4, no. 3, pp. 508–517, Sep. 2021, doi: [10.1007/s41918-021-00097-4](https://doi.org/10.1007/s41918-021-00097-4).
- [10] T. N. Veziroğlu and S. Şahin, "21st Century's energy: Hydrogen energy system," Energy Convers Manag, vol. 49, no. 7, pp. 1820–1831, Jul. 2008, doi: [10.1016/j.enconman.2007.08.015](https://doi.org/10.1016/j.enconman.2007.08.015).
- [11] A. Mohammadi and M. Mehrpooya, "Thermodynamic and economic analyses of hydrogen production system using high temperature solid oxide electrolyzer integrated with parabolic trough collector," J Clean Prod, vol. 212, pp. 713–726, Mar. 2019, doi: [10.1016/j.jclepro.2018.11.261](https://doi.org/10.1016/j.jclepro.2018.11.261).
- [12] J. Sanz-Bermejo, V. Gallardo-Natividad, J. González-Aguilar, and M. Romero, "Coupling of a Solid-oxide Cell Unit and a Linear Fresnel Reflector Field for Grid Management," Energy Procedia, vol. 57, pp. 706–715, 2014, doi: [10.1016/j.egypro.2014.10.226](https://doi.org/10.1016/j.egypro.2014.10.226).

- [13] A. A. AlZahrani and I. Dincer, "Design and analysis of a solar tower based integrated system using high temperature electrolyzer for hydrogen production," *Int J Hydrogen Energy*, vol. 41, no. 19, pp. 8042–8056, May 2016, doi: [10.1016/j.ijhydene.2015.12.103](https://doi.org/10.1016/j.ijhydene.2015.12.103).
- [14] A. Houaijia, M. Roeb, N. Monnerie, and C. Sattler, "Solar power tower as heat and electricity source for a solid oxide electrolyzer: a case study," *Int J Energy Res*, vol. 39, no. 8, pp. 1120–1130, Jun. 2015, doi: [10.1002/er.3316](https://doi.org/10.1002/er.3316).
- [15] A. Mohammadi and M. Mehrpooya, "Techno-economic analysis of hydrogen production by solid oxide electrolyzer coupled with dish collector," *Energy Convers Manag*, vol. 173, pp. 167–178, Oct. 2018, doi: [10.1016/j.enconman.2018.07.073](https://doi.org/10.1016/j.enconman.2018.07.073).
- [16] S. R. Pavlovic and V. P. Stefanovic, "Ray Tracing Study of Optical Characteristics of the Solar Image in the Receiver for a Thermal Solar Parabolic Dish Collector," *Journal of Solar Energy*, vol. 2015, pp. 1–10, Oct. 2015, doi: [10.1155/2015/326536](https://doi.org/10.1155/2015/326536).
- [17] "Knovel - MatWeb Composite Material Data Sheets (MDS) - Silicon Carbide, Reaction-Bonded, SiSiC - Knovel." Accessed: Aug. 15, 2024. [Online]. Available: [https://app.knovel.com/kn/resources/kt012UUI1C1/kpCMDS0005/html?b-q=si-sic&cid=kt012UUI1C1&include\\_synonyms=yes&page=1&q=si-sic&rcid=kpCMDS0005&sort\\_on=default](https://app.knovel.com/kn/resources/kt012UUI1C1/kpCMDS0005/html?b-q=si-sic&cid=kt012UUI1C1&include_synonyms=yes&page=1&q=si-sic&rcid=kpCMDS0005&sort_on=default)
- [18] M. Abid, T. A. H. Ratlamwala, and U. Atikol, "Performance assessment of parabolic dish and parabolic trough solar thermal power plant using nanofluids and molten salts," *Int J Energy Res*, vol. 40, no. 4, pp. 550–563, Mar. 2016, doi: [10.1002/er.3479](https://doi.org/10.1002/er.3479).
- [19] H. Weldekidan, V. Strezov, and G. Town, "Performance evaluation of absorber reactors for solar fuel production," *Chem Eng Trans*, vol. 61, pp. 1111–1116, 2017, doi: [10.3303/CET1761183](https://doi.org/10.3303/CET1761183).
- [20] C. Ophoff, M. Abuseada, N. Ozalp, and D. Moens, "Systematic approach for design optimization of a 3 kW solar cavity receiver via multiphysics analysis," *Solar Energy*, vol. 206, pp. 420–435, Aug. 2020, doi: [10.1016/j.solener.2020.06.021](https://doi.org/10.1016/j.solener.2020.06.021).
- [21] V. R. Patil, F. Kiener, A. Grylka, and A. Steinfeld, "Experimental testing of a solar air cavity-receiver with reticulated porous ceramic absorbers for thermal processing at above 1000 °C," *Solar Energy*, vol. 214, pp. 72–85, Jan. 2021, doi: [10.1016/j.solener.2020.11.045](https://doi.org/10.1016/j.solener.2020.11.045).
- [22] A. S. Kopalakrishnaswami and S. K. Natarajan, "Comparative study of modified conical cavity receiver with other receivers for solar paraboloidal dish collector system," *Environmental Science and Pollution Research*, vol. 29, no. 5, pp. 7548–7558, Jan. 2022, doi: [10.1007/s11356-021-16127-z](https://doi.org/10.1007/s11356-021-16127-z).
- [23] A. Kasaeian, A. Kouravand, M. A. Vaziri Rad, S. Maniee, and F. Pourfayaz, "Cavity receivers in solar dish collectors: A geometric overview," *Renew Energy*, vol. 169, pp. 53–79, May 2021, doi: [10.1016/j.renene.2020.12.106](https://doi.org/10.1016/j.renene.2020.12.106).
- [24] R. E. Sonntag, C. Borgnakke, and G. J. Van Wylen, *Fundamentals of thermodynamics*, 5th ed. Wiley, 1998. Accessed: Aug. 18, 2024. [Online]. Available: <https://cir.nii.ac.jp/crid/1130282271577271936.bib?lang=en>
- [25] D. O. Kipp, *MatWeb Composite Material Data Sheets (MDS)*. MatWeb, LLC., 2010. [Online]. Available: <https://app.knovel.com/hotlink/toc/id/kpCMDS0005/matweb-composite-material/matweb-composite-material>
- [26] Inc. ANSYS, "ANSYS Fluent Material Library," 2024, ANSYS, Inc.: 2024 R1.
- [27] K. Suzuki et al., "Thermal and mechanical properties of CeO<sub>2</sub>," *Journal of the American Ceramic Society*, vol. 102, no. 4, pp. 1994–2008, Apr. 2019, doi: [10.1111/jace.16055](https://doi.org/10.1111/jace.16055).
- [28] mol K. C J and mol K. H, "The NBS Tables of Chemical Thermodynamic Properties," CRC Press, 1982.
- [29] D. O. Kipp, *MatWeb Ceramics Material Data Sheets (MDS)*. MatWeb, LLC., 2021. [Online]. Available: <https://app.knovel.com/hotlink/toc/id/kpMWCMD506/matweb-ceramics-material/matweb-ceramics-material>
- [30] C. Heisel, C. Caliot, T. Chartier, S. Chupin, P. David, and D. Rochais, "Digital design and 3D printing of innovative SiC architectures for high temperature volumetric solar receivers," *Solar Energy Materials and Solar Cells*, vol. 232, p. 111336, Oct. 2021, doi: [10.1016/j.solmat.2021.111336](https://doi.org/10.1016/j.solmat.2021.111336).

- [31] M. Cagnoli, L. Savoldi, R. Zanino, and F. Zaversky, "Numerical evaluation of an innovative cup layout for open volumetric solar air receivers," 2016, p. 030007. doi: [10.1063/1.4949059](https://doi.org/10.1063/1.4949059).
- [32] National Institute of Standards and Technology (NIST), "REFPROP (Reference Fluid Thermodynamic and Transport Properties)," 2018, National Institute of Standards and Technology: 10.0.
- [33] G. D. Raithby and E. H. Chui, "A Finite-Volume Method for Predicting a Radiant Heat Transfer in Enclosures With Participating Media," J Heat Transfer, vol. 112, no. 2, pp. 415–423, May 1990, doi: [10.1115/1.2910394](https://doi.org/10.1115/1.2910394).
- [34] E. H. Chui and G. D. Raithby, "COMPUTATION OF RADIANT HEAT TRANSFER ON A NONORTHOGONAL MESH USING THE FINITE-VOLUME METHOD," Numerical Heat Transfer, Part B: Fundamentals, vol. 23, no. 3, pp. 269–288, Apr. 1993, doi: [10.1080/10407799308914901](https://doi.org/10.1080/10407799308914901).